USAARL Report No. 2001-05

Visual Search Performance in HMDs With Partial Overlapped Binocular Fields-of-View

By Victor Klymenko, Thomas H. Harding, Howard H. Beasley (UES); and Clarence E. Rash (USAARL)

Aircrew Health and Performance Division

June 2001

U S A A R L

U.S. Army Aeromedical Research Laboratory

Notice

Qualified requesters

Qualified requesters may obtain copies from the Defense Technical Information Center (DTIC), Cameron Station, Alexandria, Virginia 22314. Orders will be expedited if placed through the librarian or other person designated to request documents from DTIC.

Change of address

Organizations receiving reports from the U.S. Army Aeromedical Research Laboratory on automatic mailing lists should confirm correct address when corresponding about laboratory reports.

Disposition

Destroy this document when it is no longer needed. Do not return it to the originator.

Disclaimer

The views, opinions, and/or findings contained in this report are those of the author(s) and should not be construed as an official Department of Army position, policy, or decision, unless so designated by other official documentation. Citation of trade names in this report does not constitute an official Department of the Army endorsement or approval of the use of such commercial items.

Unclassified

SECURITY CLASSIFICATION OF THIS PAGE

REPORT DOCUMENTATION PAGE

Form Approved
OMB No. 0704-0188

1a. REPORT SECURITY CLASSIFICATION
Unclassified

1 b. RESTRICTIVE MARKINGS

2a. SECURITY CLASSIFICATION

3. DISTRIBUTION / AVAILABILITY OF REPORT
Approved for public release, distribution unlimited

2b. DECLASSIFICATION / DOWNGRADING

4. PERFORMING ORGANIZATION REPORT NUMBER(S)
USAARL Report No. **2001-05**

5. MONITORING ORGANIZATION REPORT NUMBER(S)

6a. NAME OF PERFORMING ORGANIZATION
U.S. Army Aeromedical Research Laboratory

6b. OFFICE SYMBOL *(If*
MCMR-UAD

7a. NAME OF MONITORING ORGANIZATION
U.S. Army Medical Research and Materiel Command

6c. ADDRESS (City, *State, and ZIP Code)*
P.O. Box 620577
Fort Rucker, AL 36362-0577

7b. ADDRESS *(City, State, and ZIP Code)*
504 Scott Street
Frederick, MD 21702-5012

8a. NAME OF FUNDING / SPONSORING ORGANIZATION

8b. OFFICE SYMBOL *(If*

9. PROCUREMENT INSTRUMENT IDENTIFICATION NUMBER

8c. ADDRESS *(City, State, and ZIP Code)*

10. SOURCE OF FUNDING NUMBERS

PROGRAM ELEMENT NO.	PROJECT NO.	TASK NO.	WORK UNIT ACCESSION NO.
622787	879	P	DA336445

11. TITLE *(Include Security Classification)*
(U) Visual search performance in HMDs with partial overlapped binocular fields-of-view

12. PERSONAL AUTHOR(S)
Victor Klymenko, Thomas H. Harding, Howard H. Beasley, Clarence E. Rash

13a. TYPE OF REPORT	13b. TIME COVERED FROM TO	14. DATE OF REPORT *(Year, Month,*	15. PAGE COUNT
Final		**2001** June	**25**

16. SUPPLEMENTAL NOTATION

17. COSATI CODES

FIELD	GROUP	SUB-GROUP
23	02	
20	06	

18. SUBJECT TERMS *(Continue on reverse if necessary and identify by block number)*
helmet-mounted displays, partial binocular overlap, field-of-view

19. ABSTRACT *(Continue on reverse if necessary and identify by block number)*
A helmet-mounted display (HMD) with a partial binocular overlap field-of-view (FOV) is slated for use with the Army's new RAH-66 Comanche helicopter in order to increase the available size of the FOV. The current investigation examined how three FOV configurations affect performance in a visual search task under demanding viewing conditions. Performance was measured by response time and accuracy in the full overlap FOV, the convergent partial overlap FOV, and the divergent partial overlap FOV. Twenty-one aviators were required to visually scan for and identify a number out of eight alphanumerics randomly positioned in a randomly cluttered FOV as quickly as possible while minimizing errors. In general, the fastest response times (RTs) were to targets in the full overlap FOV compared to the partial overlap FOVs.The RT performance data were not disconfirmed by the accuracy data, that is, there was no speed-accuracy trade-off in the data, meaning, accuracy was not deferentially substituted for response speed across conditions. There were no significant differences in accuracy for the three FOV conditions.

20. DISTRIBUTION / AVAILABILITY OF
☒ UNCLASSIFIED/UNLIMITED ☐ SAME AS RPT. ☐ DTIC USERS

21. ABSTRACT SECURITY CLASSIFICATION
Unclassified

22a. NAME OF RESPONSIBLE INDIVIDUAL	22b. TELEPHONE *(Include Area*	22c. OFFICE SYMBOL
Chief, Science Support Center	(334) 255-6907	MCMR-UAX-SS

DD Form 1473, JUN 86 *Previous editions are obsolete.*

SECURITY CLASSIFICATION OF THIS PAGE
Unclassified

Acknowledgments

We thank Dr. William McLean for his review. This work was completed under the U.S. Army Medical Research and Development Command Contract No. DAMD17-91-C-1081.

Table of contents

Table of contents (continued)

List of figures

Page

List of tables

Introduction

The size of a helmet-mounted display's (HMD's) field-of-view (FOV) is the size of the visual world available to an Army helicopter pilot via an imaging sensor. A binocular partial overlap HMD is slated for use with the Army's new RAH-66 Comanche helicopter. Currently, monocular HMDs are used in the Army's AH-64 Apache helicopter. The Comanche's HMD will present the binocular FOV in a partial overlap configuration rather than a full overlap configuration. In the full overlap configuration, the images presented to each eye, the monocular fields, are identical views of the visual world where the FOV consists of a single binocular region. In the partial overlap configuration, the FOV consists of the central binocular overlap region seen by both eyes, and two flanking monocular regions, each seen by one eye. How effective is this visual interface? We briefly describe the relevant differences between normal unaided vision and vision with a binocular HMD and briefly review the visual effects of binocular HMDs and how visual performance might be affected. Our concern is how these displays might affect the visual tasks required of military pilots. Our study compares visual search performance under different HMD FOV configurations.

Binocular human vision normally consists of an overlapping divergent FOV where the overall horizontal FOV is approximately 200 degrees of visual angle (when viewed straight ahead), with each eye's monocular field around 120 degrees of visual angle. The two monocular fields combine to produce an FOV consisting of three regions. The central binocular region, which both eyes can see, is approximately 120 degrees, and the two flanking monocular regions, each seen exclusively by a single eye, are each approximately 40 degrees. The FOV is described as divergent because the right eye sees the monocular region to the right of the common binocular region and the left eye sees the monocular region to the left of this region (Figures 1 and 2).

The size of the monocular fields an HMD can present to each eye is limited by current technology due to the weight and size of the HMD oculars and the need for adequate eye clearance. Therefore, the size of the FOV in a full overlap configuration is limited to the size of each monocular field. Small FOVs can be detrimental to the visual tasks required of military pilots (Kenyon and Kneller, 1993; Osgood and Wells, 1991; Wells, Venturino, and Osgood, 1989; Wolpert, 1990; Jennings and Dion, 1997; Jennings et al., 1997; and Klymenko et al., 1999). The Comanche program has settled on the partial overlap method to increase the FOV. Relative to full overlap, the horizontal FOV of HMDs can be increased, without increasing the size of the monocular fields, by combining them so that they binocularly overlap only partially (Melzer and Moffitt, 1989, 1991). In the HMD's FOV, this artificial partial overlap configuration can be either divergent as in normal vision, or it can be convergent. In the divergent partial overlap configuration, as in normal vision, the right eye will see the monocular region to the right of the binocular overlap region and the left eye will see the monocular region to the left. The resulting visual regions will be smaller than they are in normal vision because the HMD's monocular fields are smaller than each eye's normal view. In the convergent partial overlap configuration, contrary to the divergent partial overlap configuration, the right eye will see the monocular region to the left of the binocular overlap region and the left eye will see the

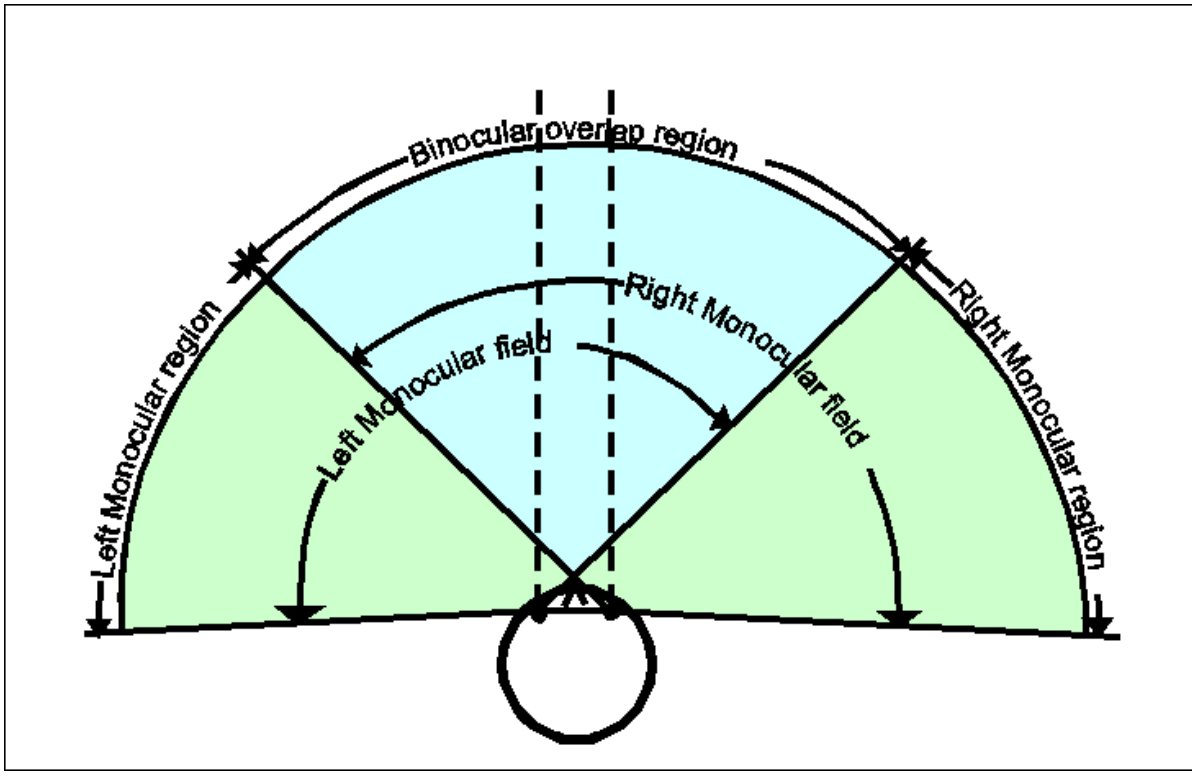

Figure 1. In normal unaided vision, the two monocular fields are partially overlapped producing a divergent FOV consisting of three regions, the central binocular overlap region and two flanking monocular regions.

monocular region to the right. In a full overlap configuration where both monocular fields display the same central binocular region, the FOV is one binocular region the size of a monocular field.

Thus, to overcome the limited size of the monocular fields, the partial overlap method increases the available FOV in the HMD without increasing the size and weight of the HMD or losing central resolution. However, the partial overlap method has been a source of ongoing concern (Alam et al., 1992; Edgar et al., 1991; Kruk and Longridge, 1984; Landau, 1990; Moffitt, 1989, 1991; and Moffitt and Melzer, 1991). One consequence of partial overlap is the effect known as luning (Figure 2), a subjective darkening of the monocular regions near the binocular overlap border (Moffitt, 1989; Klymenko et al., 1994b). Luning can lower the visibility of stimuli as well as distract the pilot using the HMD. Partial overlap can also cause visual fragmentation, which refers to the segmented phenomenal appearance of the display as three distinct regions instead of the perceptually unitary FOV one should see (Klymenko et al., 1994a). Luning and fragmentation tend to be greater in divergent than in convergent displays (Klymenko et al., 1994a,b). This is because the partial overlap FOV of the HMD is smaller than the FOV in normal unobstructed vision. This results in both the central binocular region and the two flanking monocular regions falling into a visual area that is normally completely binocular. Visual processes such as binocular rivalry and dichoptic competition in the monocular regions can then be experienced as luning and visual fragmentation of the FOV. (See discussions in

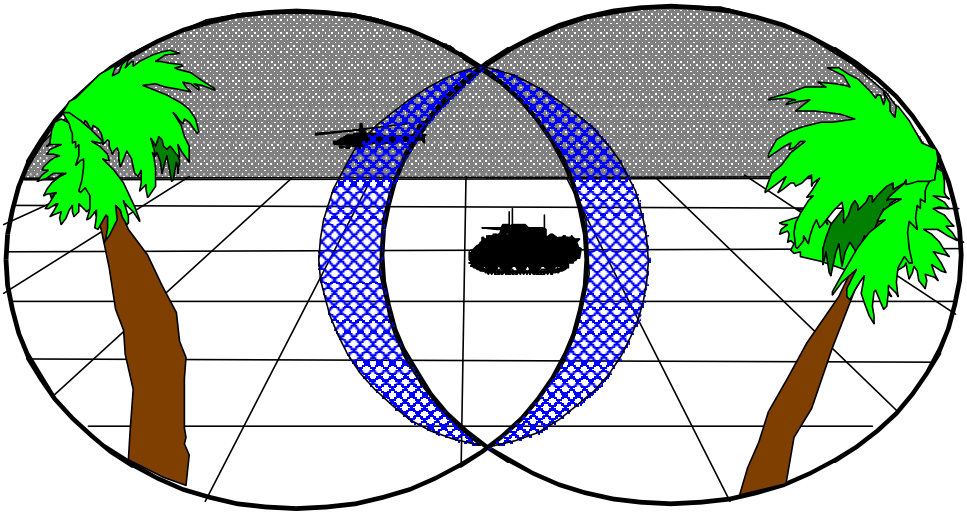

Figure 2. Pilot's view of visual world in an HMD with a partially binocular overlapped FOV. Note the exaggerated presence of luning at the overlap borders.

Klymenko et al., 1994a,b,c.). In addition to these phenomenal effects, targets near threshold are harder to see in the monocular regions of partial overlap FOVs (Klymenko et al, 1994c). The visibility of targets, and the visual world in general, seen in the HMD's FOV is, of course, of paramount importance to military aviators. Though these effects were relatively small in terms of the contrast needed to identify the target, they were, nevertheless, clear cut and systematic. One reason for the reduced target visibility in partial overlap FOVs is the dichoptic competition between the two eyes due to conflicting visual information. This includes a general visual system effect of binocular rivalry (and alternating monocular dominance) between the two eyes and a specific stimulus effect due to the binocular overlap border in the display. Another reason is the general reduction in sensitivity due to the binocular combination of the two disparate images in the monocular regions. For more extended discussions, see Klymenko et al. (1994a,b,c). The question is: Are these perceptual effects likely to affect general visual performance?

In Klymenko et al. (1999), we found that visual performance, as measured by response time to target acquisition, and accuracy of target acquisition is, in general, poorer in the monocular regions of partial overlap FOVs, more so in the divergent than the convergent partial overlap FOV. In that study, target positions were constant. The current study, incorporating a number of methodological changes, is a preliminary investigation of visual search performance where target locations are variable and the observer must scan the display to find the target. The study was designed to gain more understanding of the real world impact of FOV designs on general visual performance by using a visual search task under the psychological constraints experienced in aviation. These include time pressure, uncertainty of the specific target and of its location, and a randomly cluttered background. Observers needed to visually scan the FOV to search for the target. Aviation is an attention-demanding (high mental workload) environment with a high

rate of visual information throughput where visual inspection time is often limited and the eyes need to continually scan an FOV. This is a stimulus environment that often taxes the visual performance of the human perceiver. Under operational conditions, human performance may be compromised by the partial overlap FOV design. The performance decrements with these HMDs may become critical in attention demanding environments such as military aviation. This study assesses the effects of these FOV configurations on visual performance under demanding viewing conditions.

Visual search experiment

In this exploratory study, the task was to search through a group of randomly located alphanumeric symbols and identify the target (one of five possible numbers) from among similar distractors (letters) in each trial display as quickly as possible. Response time and accuracy were the measures of visual performance. The target could be any one of several numbers, and the distractors could each be any one of several letters. The task was to identify which number was present in each display. To make the task more difficult, the target number and distractor letters (collectively, the alphanumeric symbols), were randomly oriented, and unlike the previous study (Klymenko et al., 1999), their locations were randomized, rather then being in an array of fixed positions. Also, on half the trials, the alphanumerics were spatially blurred to test the effect of this factor. Each display contained random clutter in the form of randomly located ellipses of random size and orientation. Automated feedback was given to motivate subjects to perform at maximum capacity. Also, we used smooth temporal onsets for the symbols, as abrupt onsets make stimuli strong dichoptic competitors (Kaufman, 1963; 1964) and therefore could mask relevant differences among conditions.

We had four general hypotheses: One, the FOV factor would effect target acquisition, with subjects exhibiting better performance in full overlap than in partial overlap FOVs and better performance in convergent partial overlap than divergent partial overlap FOVs. Two, performance would depend on the target position in the FOV. It was expected that performance would be worst in the monocular regions of partial overlap FOVs. Because of the change from the previous study, we eliminated response bias as a factor, therefore performance at different positions is now directly comparable. Three, we conjectured that blurred targets might cause poorer performance in monocular regions because blurring reduces a stimulus' strength in dichoptic competition (Kaufman, 1963,1964). Four, we assumed performance would improve over time.

In this preliminary study, we looked at how the type of FOV, the position of a stimulus in the FOV and the spatial blurring of the stimulus affected visual performance, and how visual performance is maintained over time. The task was to visually search the FOV for a series of displays, and in each display, identify the target as quickly as possible without making errors.

Method

Subjects

Twenty-one student army aviators, 20 males and 1 female, voluntarily took part in the experiment. This population had passed Class II flight physical vision tests. All had 20/20 unaided or better Snellen acuity. The mean age was 26.5 (SD =2.8), ranging from 21 to 30. Two additional subjects were not included in these data because the testing was interrupted due to computer and equipment problems.

Equipment

The equipment consisted of three major components: a Hewlett-Packard HP-98731 Turbo-SRX computer graphics workstation used to generate the visual stimuli, a custom optical table configuration used to optically direct the visual stimuli from the workstation monitor to a pair of viewing binoculars, and a subject booth. The booth was a light-proof enclosure behind the binoculars where the subject viewed the stimuli via the binoculars and responded via an HP response keypad, the "buttonbox." The HP-98731 Turbo-SRX computer graphics workstation consisted of a 19-inch color Trinitron monitor (1280 x 1024 pixels) for presenting visual stimuli and a computer for generating the stimuli and recording the responses. Connected to the workstation were the experimenter's terminal to allow the experimenter to run the experimental programs and monitor the progress of each experimental session, and the buttonbox to allow the subject to respond to the visual stimulus presentations.

The optical table configuration consisted of a 4-foot x 6-foot optical table, with the workstation monitor mounted at one wide side of the table, and eight front-surfaced mirrors mounted on the table to direct the visual image--the optical train--to a pair of viewing binoculars mounted on the other wide side of the table (Figure 3). The mirrors allowed the independent presentation of two channels, one to each ocular of the binoculars, from the same monitor. Through the binoculars, the image on the top half of the monitor was seen by the left eye, and the
image on the bottom half of the monitor was seen by the right eye. The 7x50 binoculars were mounted within a fixture which allowed the interpupillary distance (IPD) to be adjusted for each subject. Affixed on the front of the binoculars were auxiliary focusing lenses to focus the magnified image. A light baffle in front of the monitor between the two optical paths was positioned to prevent cross talk between the two image channels. Optical convergence was adjusted for two meters. The focus was between one and two meters across the FOV to compensate for slight field aberrations in the binoculars and possible slight inducement of instrument myopia. The two mirrors, L4 and R4 in Figure 3, mounted directly in front of the binoculars, were movable to allow adjustments corresponding to the IPD settings of the binoculars. The images seen through each ocular of the binoculars were 50 degrees of visual angle corresponding to 1280 pixels. The spatial resolution of the display was 25.6 pixels per degree of visual angle as seen through the binoculars. The temporal resolution, or frame rate of the monitor, was 60 Hz noninterlaced. The luminance resolution was 256 driving levels. The driving level to luminance conversions are given below. The 7x50 binoculars have a vertex

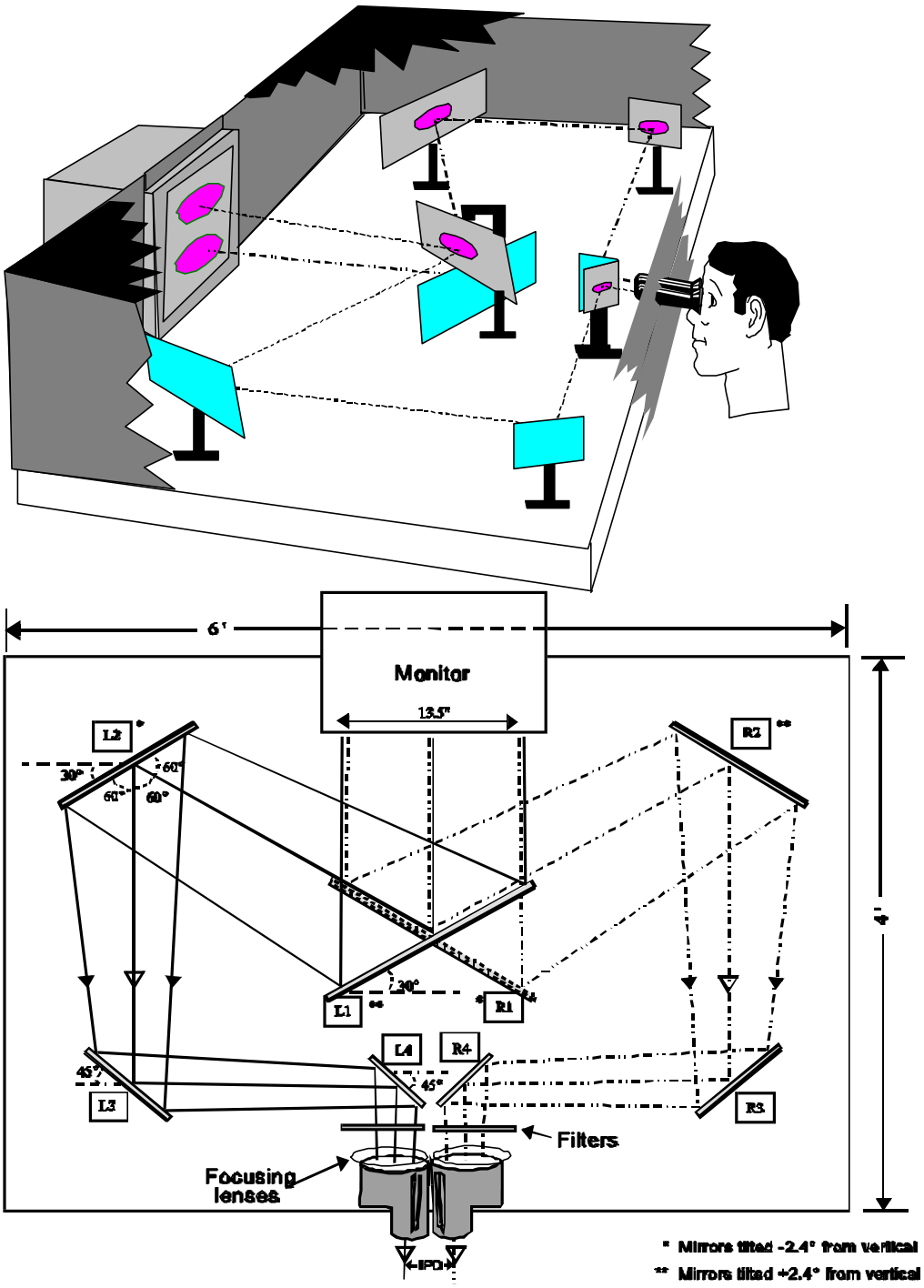

Figure 3. Perspective and schematic illustrations of the optical table configuration consisting of the monitor, eight mirrors, focusing lenses, and binoculars.

distance of 27 mm and an exit pupil diameter of 7.14 mm. The subject, within reach of the buttonbox, was seated at a chin rest in the light-proof subject booth in front of the binoculars. Except for the stimuli viewed through the binoculars, the subject was in darkness.

Stimuli

The stimuli consisted of a series of computer-generated displays, where each display was in one of three FOV configurations. Each FOV contained eight alphanumeric symbols, all sharp or all blurred, seven of which were letters and one a numerical digit, which was the target. The particular letters and the particular number, the position of the target, the vertical location of all symbols, and each symbol's orientation were randomized. Also, each FOV contained 6 small crosses for fusion locks and 60 randomly-sized and randomly-positioned ellipses (half light grey and half dark grey) for background clutter. For each trial, two seconds after the FOV appeared, the eight symbols slowly appeared, taking an additional 0.8 seconds to go from invisible to maximum visibility. Stimulus details are given below, and shown in Figures 4-7. Stimulus luminance values displayed on the screen, in terms of the 0-255 digital driving levels, took on values between 0 (black, 0.01 fL) through 64 (dark grey, 1.33 fL), 128 (neutral grey, 6.65 fL) to 192, (light grey, 16.81 fL). Half of the ellipses were light grey and half were dark grey. The FOV background was neutral grey. The area outside the FOV was black, as were the fusion locks.

The original sharp symbols were predefined as black, and the blurred symbols were sharp symbols modified by the blurring algorithm which causes the luminance of a symbol's pixels (and neighboring pixels) to vary in a complex way with different pixels taking on different values. The resulting values were between the pixel's original pre-blurred (black) value and the values of the pixel's local surround---some combination of black and neutral grey pixels. Then the symbol values were modified by lookup tables before display in order to present a smooth temporal onset. In essence, what this did was to start off the symbols as invisible and then smoothly increase the contrast by making the symbol darker to a value where they were clearly visible. This is described in detail below.

Fields-of-view

The total FOV was a rectangular area, 32.8 degrees of visual angle horizontal (840 pixels) by 10 degrees of visual angle vertical (256 pixels) (Figures 4-7). The subjects saw the total FOV via the monocular fields presented to each eye. The monocular fields were each 23.4 degrees of visual angle horizontal (600 pixels) by the full vertical extent. The FOV configurations differed in how the two monocular fields overlapped, and consequently the total FOV presented to both eyes. In the full overlap FOV configuration, each eye's monocular field displayed the same central portion of the total FOV, so that the FOV seen by the subject was binocular and consisted of the central 23.4 degrees of the total FOV. In the divergent partial overlap FOV, the right eye's monocular field was the right-most 23.4 degrees and the left eye's monocular field was the left-most 23.4 degrees of the total FOV; therefore, the FOV seen by the subject consisted of a central binocular overlap region of 14.1 degrees and two flanking monocular regions, each of

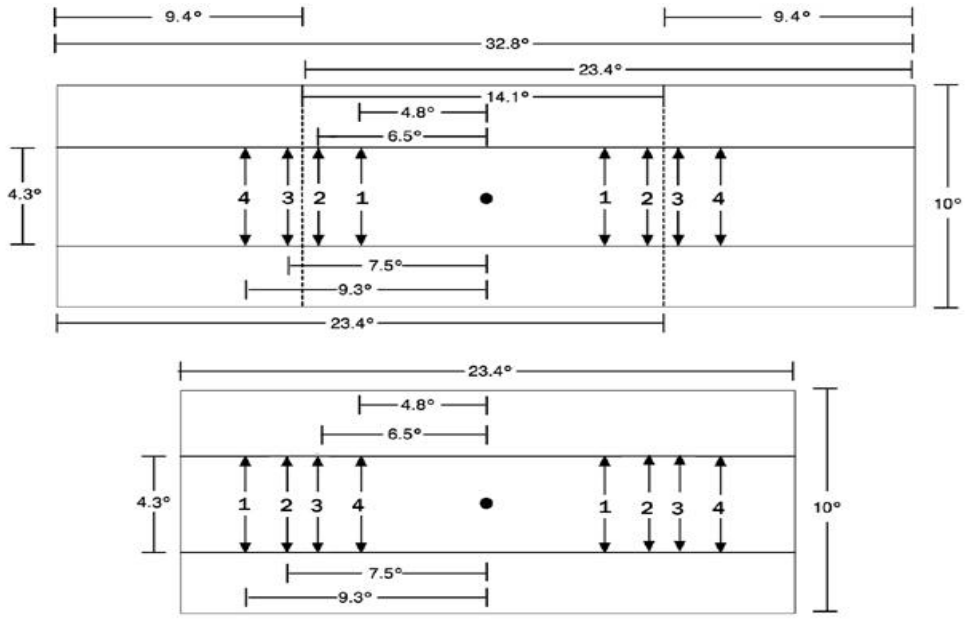

Figure 4. FOV dimensions. Four target positions in degrees of visual angle from the center are shown on the right and four symmetrical positions are shown on the left. The top shows a partial overlap FOV and the bottom shows a full overlap FOV.

9.4 degrees. In the convergent partial overlap FOV, the right eye's monocular field was instead the left-most 23.4 degrees and the left eye's monocular field was the right-most 23.4 degrees of the total FOV. Again, the FOV seen by the subject consisted of a central binocular overlap region of 14.1 degrees and two flanking monocular regions, each of 9.4 degrees. In the divergent case, the right eye saw the flanking monocular region to the right and the left eye saw the flanking monocular region to the left, while in the convergent case these were reversed, that is, the left eye saw the right monocular region and the right eye saw the left region (Figure 4).

In both partial overlap conditions, the FOV seen by the subject was the full 32.8 degrees of the total FOV. This FOV consisted of a 14.1 degree central binocular region and two flanking 9.4 degree monocular regions, with each eye seeing the monocular regions as described. In the full overlap condition, the FOV seen by the subject was the central 23.4 degree portion of the total FOV. In the full overlap condition, the binocular region was larger than in the partial overlap conditions, while in the partial overlap conditions, an enlarged FOV is seen with a smaller binocular region. In all the conditions, the monocular fields were the same size.

These FOVs were presented by drawing each eye's monocular field separately on the top and bottom halves of the monitor and directing the images to each eye's view through the binoculars via the optical table configuration.

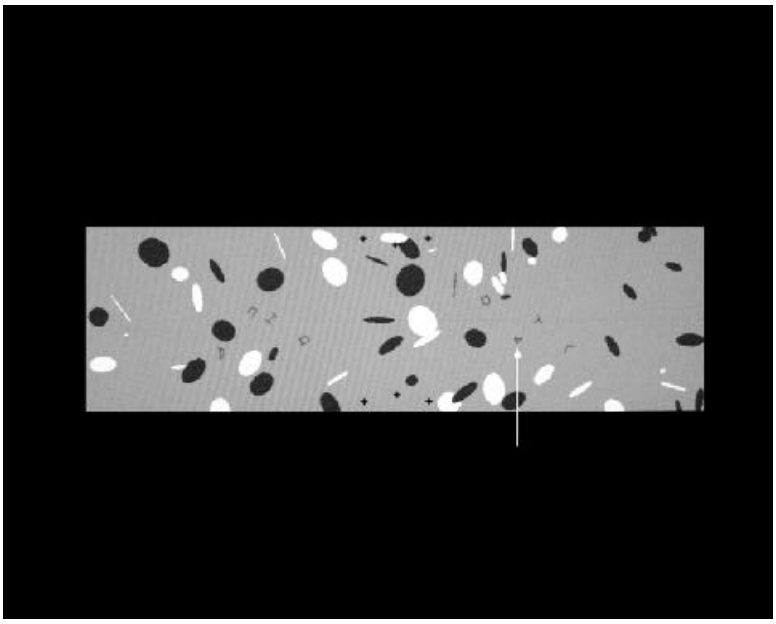

Figure 5. Example of a total FOV with blurred symbols. Target is the numeral "4" indicated by an arrow.

The subjects require similar stimuli common to both eyes to prevent disjunctive eye movements in order to binocularly fuse images properly and to avoid the image slippage which leads to the binocular overlap of inappropriate regions. To ensure proper binocular locking of the monocular fields and to provide a way to monitor binocular fusion, fusion locks were present in each display. These were six crosses, three in the upper center of the total FOV and three in the lower center. Subjects were told that they should see three crosses above and below the center of each display. If they saw more, then the images were not properly fused and they should tell the experimenter. This did not occur. With the background clutter described below, there were ample binocular stimuli to prevent slippage. Each shaft of the crosses was 8 pixels long by 2 pixels wide. Center crosses were 25 pixels from the top and bottom of the FOV, and flanking crosses were located 44 pixels to the right and left of the center and 16 pixels from the top and bottom of the FOV (Figures 5-7).

Alphanumeric symbols and targets

In each display, one of eight alphanumeric symbols was the target number, and the remaining seven were nontarget letters. Alphanumeric symbols were all in "stick figure" font, or font number 1, predefined in the Hewlet-Packard Starbase computer graphics language. Letters were all capitals, and all alphanumeric symbols were originally defined within a 16 by 16 pixel symbol square (0.6 by 0.6 degrees of visual angle). Alphanumerics were initially defined as 0 driving levels (black). The orientation of each symbol was randomized by rotating the symbol

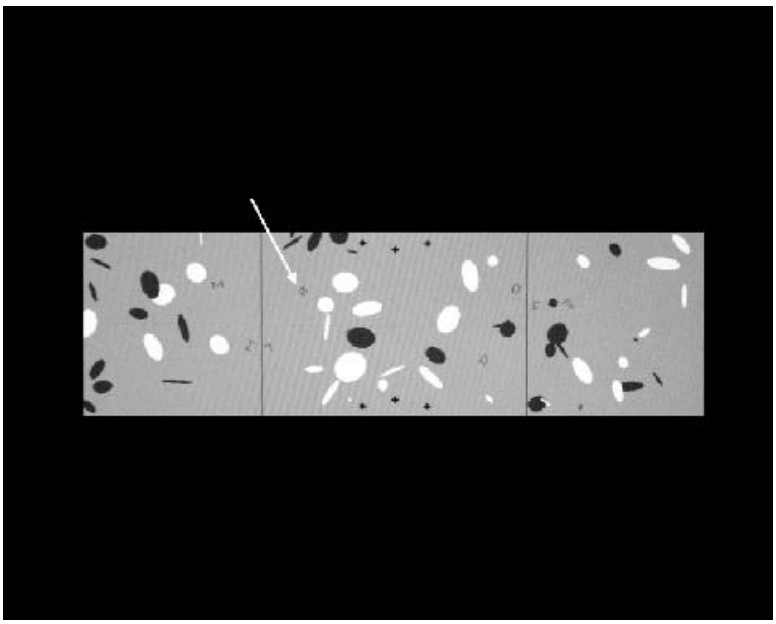

Figure 6. The total FOV divided into the three regions seen in the partial overlap displays, the central binocular overlap region and the two flanking monocular regions. The vertical lines were not present in the displays. The left monocular field consists of the left and central regions, and the right monocular field consists of the central and right regions. In the divergent FOVs, the left eye saw the left monocular field, and the right eye saw the right monocular field. In the convergent FOVs, the left eye instead saw the right monocular field, and the right eye saw the left monocular field. In this display the symbols are sharp. Target is the numeral "2" indicated by the arrow.

randomly from 0 to 360 degrees. The blurred symbols were spatially blurred as follows. The original symbol square consisted of black symbol pixels and non-symbol pixels. The symbol pixels and adjacent non-symbol pixels were defined as the blur zone. This blur zone included any symbol pixel, that is a pixel that contained part of the alphanumeric symbol, and any non-symbol pixel that was adjacent to a symbol pixel, adjacency defined as the eight contact pixels. The pixels in the blur zone were then filtered by a 3 by 3 Gaussian kernel. This means that for each blur zone pixel, the old driving level was replaced by a new driving level, which was the weighed average of the old value and the driving levels of the eight pixels around it. The kernel weights were as follows where the central "12" represents the weight of the old driving level:

1	4	1
4	12	4
1	4	1

The symbol edges were softened by blurring the symbol into the FOV. The blurred symbols contained more pixels with smoother transitions between symbol and background.

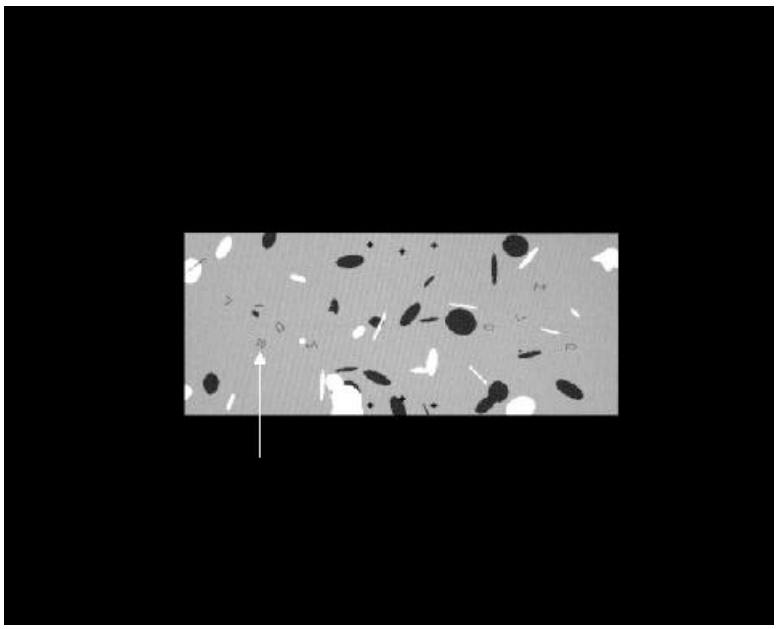

Figure 7. A full overlap FOV where both monocular fields consist of the same central portion of the total FOV. The symbols are sharp. Target is the numeral "2" indicated by the arrow.

All symbols, sharp and blurred, gradually appeared in the FOV to avoid sharp temporal onsets. This was implemented by passing the symbol (blurred or sharp) through a series of lookup table functions, one function for each frame of the temporal sequence. In the lookup table function, each original input driving level in the symbol was changed to an output displayed driving level. Cycling through the set of functions caused the original symbol's luminance to change smoothly from invisible, where all the pixels were equal to the background of the FOV (128 driving levels) to clearly visible, which was 45 driving levels in the sharp symbols, and in the blurred symbols, the pixel values were based on the pixel values resulting from the original blurring. The temporal onset was done by the following lookup table equation:

$$y = x * \tan(\text{angle}) - (128 * \tan(\text{angle})) + 128,$$

where x = input pixel driving level; y = output pixel driving level; and angle = 0 to 30 degrees in steps of 1.25 degrees.

Angle represents the slope of the input-output lookup table function which changed every two frames. At 45 degrees, all displayed driving levels (y) would be equal to original input driving levels (x), zero in the case of the sharp symbols and the original blurred values in the case of the blurred symbols. At 0 degrees, all output driving levels (y) equaled 128, where the entire symbol was the same driving level as the FOV background and therefore invisible. Forty-eight frames, taking 0.8 seconds, presented the transition from invisible (0 degrees) to fully visible (30 degrees) by incrementing from 0 to 30 degrees in steps of 1.25 degrees with 2 frames per step.

The symbol positions in terms of degrees of visual angle from the center of the symbol to the center of the FOV were located as shown in Figure 4. Four positions were to the right of center, and four symmetrical positions were to the left of center. Horizontally, the symbols were located as follows. The positions numbered 1 were 123 pixels (4.8 degrees of visual angle) to the right and left of center. The positions numbered 2 were 167 pixels (6.5 degrees of visual angle) to the right and left of center. Positions numbered 3 were 193 pixels (7.5 degrees of visual angle) to the right and left of center, and positions numbered 4 were 237 pixels (9.3 degrees of visual angle) to the left and right of center. The edge of the symbols in positions 2 and 3 were two pixels away from the adjacent binocular overlap border. The position of each individual symbol was vertically randomized; it could be located with equal probability vertically anywhere within the central 110 pixels high region (4.3 degrees of visual angle).

Background clutter

For clutter, each display contained 30 dark grey and 30 light grey ellipses, each randomly oriented, randomly sized, and randomly located within the total FOV. The center of each ellipse could, with equal probability, be located on any pixel within the total FOV with the following stipulation. If the random placement procedure located the ellipse on or near a symbol, that is if they overlapped, then the ellipse was instead placed in a new random location. For this purpose, the symbol was defined as the original 16 x 16 pixel square and the ellipse region was defined as a square around the ellipse center with sides equal to the major axis of the ellipse. This was to avoid contaminating the results with extremely difficult to see alphanumerics on top of ellipses. The orientation of each ellipse could, with equal probability, be anywhere from 0 to 180 degrees. Ellipse size was randomized by sizing each of the two axes of each ellipse with equal probability anywhere from 1 to 44 pixels in length. Ellipses were alternatively light and dark grey, with later ellipses drawn over former ellipses.

Design and data analysis

Each trial consisted of a unique display to which the subject responded. In the experiment, 378 trials were presented in 7 blocks, where each block contained 3 FOVs, presented in random order. There were 18 trials in each FOV, where unknown to the subject, the first two of these were merely to allow the subject to acclimate to the FOV and the responses not recorded. The acclimation trial displays were random with respect to target type (sharp or blurred), target position and target number. The remaining16 trials consisted of each of the two target types, once in each of the eight positions presented in random order. For each display, the number of the target symbol was randomly 1, 2 3, 4 or 5, and each of the seven non-target letters was randomly one of twenty-two letters (the alphabet minus the letters B, E, I and S).

The experimental design for analysis was a 6 (block) x 3 (FOV) x 2 (target type) x 4 (position) repeated measures analysis of variance (ANOVA) with 144 data points for each subject for each of three response measures. The first of the seven blocks was considered practice and not included in the data analysis. Also, only the four positions to the right of center were included in the data analysis. Originally, we had intended to include all eight positions; however, we found that with some slight movement of the head for some IPDs, it was possible in some cases for the

far left symbol to fall out of the left ocular's sweet spot, i.e., become slightly blurred. In a visual search experiment subjects might inadvertently move their heads when scanning the visual field, so we eliminated some possible confounding effects of this blurring by limiting the data analysis to the four right-most positions.

The three response measures were response time (RT), number of errors, and percent errorless target acquisition. RT measures the time to hit the correct key indicating the correct target, irrespective of the number of errors. The alphanumerics appeared gradually in each FOV, taking 0.8 seconds to go from completely invisible to fully visible. The response times were measured from the halfway point, 0.4 seconds, in terms of the number of frames, which were updated every sixtieth of a second. The number of errors measures the number of wrongly acquired targets on each trial before acquiring the correct target, and it could vary from a minimum of zero to a maximum of four, as there were five possible answers. Percent errorless target acquisition measures the percentage of times subjects made no errors before target acquisition.

Procedure

Subjects were given instructions and gave informed consent for participation in the study. Each subject's interpupillary distance was measured and the equipment adjusted accordingly. The mean interpupillary distance for the 21 subjects was 61.3 mm (SD = 3.9). Subjects adjusted the chin-rest, keypad, and height of the seat for comfortable viewing of the display through the binoculars. To ensure there was no visual clipping of the FOV, or vignetting, for the area which would contain the experimental stimuli, a binocular display containing three widely spaced circles was shown. It contained the same optical convergence as the stimulus displays. The three circles were superimposed over a purple background with a white grid. There was a black circle in the center of the display, a blue circle to the right of center, and a yellow circle to the left of center. The black circle was 24 pixels in diameter and the outer two circles were 34 pixels in diameter. The outer edges of the outer circles were 668 pixels (26.1 degrees) distance from each other. The subjects were asked if they could see, without moving their head position, the entire yellow circle, the entire blue circle, and the grid surrounding each circle clearly and without vignetting when they visually scanned across the display.

In the experiment, subjects viewed a series of stimulus displays, each with eight alphanumeric symbols. The subjects were told the following: There would be eight symbols in each display, one of which was the target number. The symbols could be blurred or sharp and would be randomly oriented and randomly located. Their task for each display was to identify the number of the target, one to five, as quickly as possible, hit the appropriate key on the keypad, and avoid mistakes. Subjects could pause only during the feedback displays or "continue" displays. Five response keys in a row were assigned to each number. The middle key had a bump, so subjects could feel them in the dark.

The row of four keys above the response keys were the "next" keys, which were for continuing past the feedback displays, or the displays with the word "continue." A display with the word "continue" preceded each new FOV. To induce the need for rapid response, as well as the need to maintain accuracy, subjects were told to imagine that the target, the number, was the

enemy which would shoot them if they did not shoot it first, and the nontargets, the letters, were friendlies. Feedback displays were presented throughout the experiment to reinforce the subject's motivation to maintain maximum performance.

There were two types of feedback displays. First, seven times during the experiment, at the end of each block of trials (with three FOVs), a percentage display came on. This display showed a number with a percent sign representing the percentage of trials of the fifty-four trials of the block that were acquired on the first try without any errors. This percentage appeared on the screen to motivate the subject to maintain accuracy and avoid random guessing. Second, after every seven trails, two numbers appeared in a feedback display. The top number, followed by the word 'sec.,' was the average response time in seconds to the third decimal place that the target was acquired for the last seven trials, and the bottom number, followed by an 'X,' was the number of targets out of the last seven where there were errors before target acquisition. If there were no errors in the preceding seven trials, the word "OK" appeared instead. Seven displays was used as the average because it is not evenly divisible into the number of trials per FOV, so subjects would not be inclined to monitor their performance with respect to FOV type. The continue and the feedback displays remained on until a next key was hit. Subjects were told that for these displays they could pause if they wanted to and then initiate the next series by hitting a next key when they were ready.

Once the series of displays started, for each display, the image would remain on until the target was hit. If an error was made, a transient asterisk appeared in the center of the display and remained on as long as a wrong key was depressed. When the target number was identified by hitting the correct key, a cross appeared on the target, then the screen went blank and 1 second later a new FOV appeared, and 2 seconds later the targets began increasing contrast, reaching full visibility 0.8 seconds later.

In the experimental session, two display programs were run; one for the training and one for the experimental phase. The first ran the training phase to familiarize the subject with the task. It had FOVs with fewer trials (6 per FOV instead of 18) and, unlike the experimental phase, the symbol factors of blur and position of target were totally random, that is, random with replacement. No data were recorded. Subjects ran at least one block, and as many additional trials as they thought they needed, to fully familiarize themselves with the task and stimuli. All subjects ran between one and two blocks in this phase. Three minutes later, in the experimental phase, the second program ran seven blocks where the first block was considered practice. The blur and position factors of the acclimation trials, unlike the remaining 16 trials, were totally random. In the remaining 16 trials for which the data were recorded, the blur and position factors were random without replacement, that is, each target type-position combination appeared once. The number of the target in each trial was totally random. Subjects were not told these details; to them, all the trials were equally important and all stimulus factors were random.
There were 378 trials for each subject. The 144 nonacclimation trials of the right-most four positions of the last six blocks were included in the analysis and results reported here.

Results and conclusions

Table 1 shows the ANOVA tests for RTs. None of the interactions were significant. Three of the four main effects were significant. There was a significant block effect with RTs tending to get faster over time as shown in Figure 8, which gives the RTs over blocks for the practice block and the six test blocks for each of the three FOVs. There is some improvement over time, as one might expect, and, there is no interaction between the block factor and any other factor. The noninteraction between the block and the FOV factor is indicated by the rough parallelism of the three lines.

There was a significant main effect for FOV. Mean RT to targets in the three FOVs were as follows: divergent overlap FOV, 1.97 seconds; convergent overlap FOV, 1.93 seconds; and full overlap FOV, 1.74 seconds. The divergent FOV RT was significantly slower than the full overlap FOV, $F(1,20) = 25.03$, $p < .00007$; and the convergent FOV was significantly slower than the full overlap FOV, $F(1,20) = 20.18$, $p < .0002$; but the divergent FOV was not significantly slower than the convergent FOV, $F(1,20) = 0.77$, $p < .39$.

There was no significant main effect of target blurring. The means for blurred and non-blurred targets, respectively, were 1.88 and 1.87 seconds. Although the differing appearances of the two types of targets were apparent, the measured responses to them were virtually indistinguishable.

There was a significant main effect for position with slower RTs for targets farther away from the center. The means for positions 1 through 4, respectively, were as follows: 1.71, 1.73, 1.88 and 2.19 seconds. Figure 9 shows the RTs for each position for each of the three FOVs.

Table 2 shows the ANOVA tests for number of errors. None of the statistical tests were significant. The three FOVs over position are graphed in Figure 10.

Table 3 shows the ANOVA tests for percent errorless target acquisition. None of the tests were significant. The three FOVs over position are graphed in Figure 11. Here the perfect score of 100 percent is at the bottom of the graph to keep it in line with the other graphs where performance decrements are higher on the graph.

The two accuracy measures, in conjunction with the RT measure, show that there was no systematic speed-accuracy tradeoff, that is, no pattern of substituting speed for accuracy, or accuracy for speed, differentially across conditions.

Table 1.
RT ANOVAs

Effect	Test	F	p-level
1. Block	F (5,100)	4.58	.0008**
2. FOV	F (2,40)	14.34	.00002 **
3. Target	F (1,20)	0.07	.80
4. Position	F (3,60)	31.64	< .000001 **
5. Block x FOV	F (10,200)	0.93	.51
6. Block x Target	F (5,100)	1.17	.33
7. FOV x Target	F (2,40)	1.58	.22
8. Block x Position	F (15,300)	0.64	.84
9. FOV x Position	F (6,120)	1.92	.08
10. Target x Position	F (3,60)	0.05	.98
11. Block x FOV x Target	F (10,200)	1.13	.34
12. Block x FOV x Position	F (30,600)	1.12	.31
13. Block x Target x Position	F (15,300)	1.51	.10
14. FOV x Target x Position	F (6,120)	1.01	.42
15. Block x FOV x Target x Position	F (30,600)	0.98	.50

** = $p < .01$.

In our previous study (Klymenko et al., 1999), using response time and accuracy of target acquisition under different FOVs in a different design, position was confounded with keystroke movements; i.e., subjects responded to the position of the target with a key associated with that position. In the current study, each key was associated with a particular target number, rather than position, thereby eliminating response bias as a factor. Differences between positions here can therefore be attributed solely to the stimulus (visual) differences between positions.

One can see that, overall, target acquisition is fastest in the full overlap FOV, and slower in the two partial overlap FOV conditions.

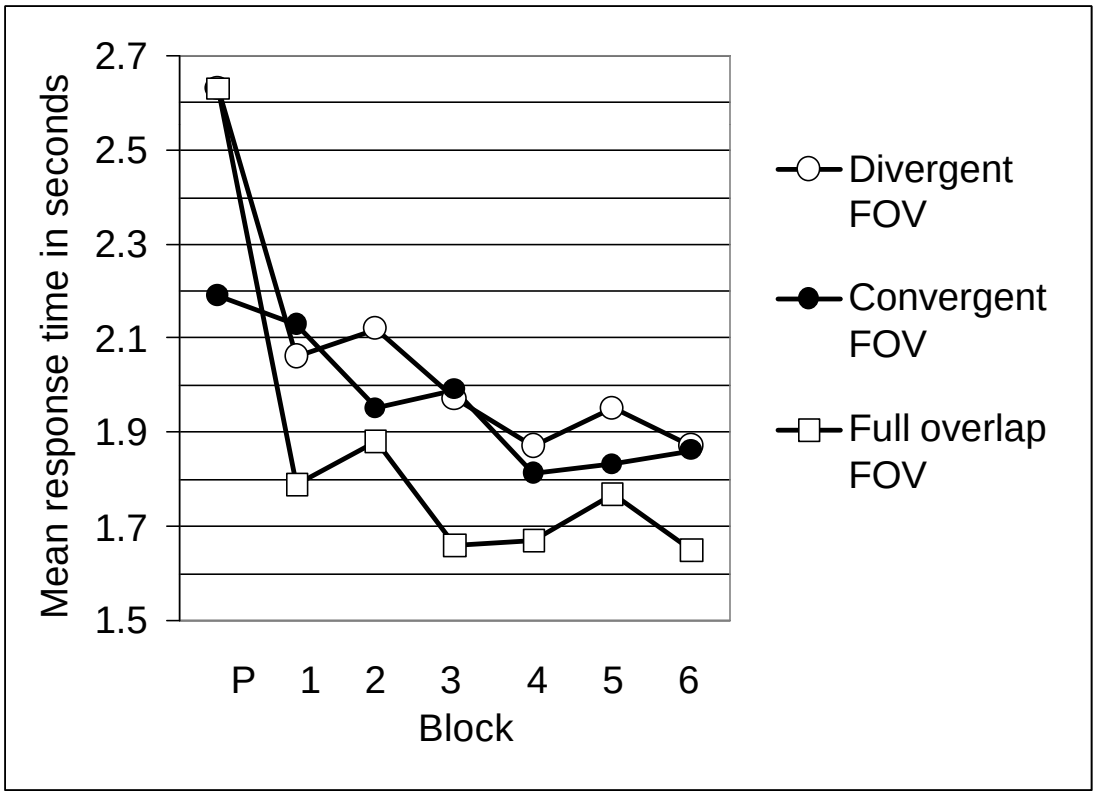

Figure 8. Mean RT to acquire target (FOV x Block). P is the practice block.

As described previously, the positions differ categorically from each other in that positions 3 and 4 are monocular in the convergent and divergent FOVs and binocular in the full overlap FOV, and positions 1 and 2 binocular in all cases. The graphed data in Figures 9-11 do not show any clear (statistically significant) pattern of changes across the boundary between positions 2 and 3 for the overlap FOVs. Distance appears to be the important factor with these suprathreshold stimuli. Separating distance and the effect of the overlap border requires additional research and more statistical power. Because the severest luning in the monocular border regions is just outside the binocular border, one might have expected peaks in the RTs for position 3. This may not have occurred here, possibly due to the attenuating effect on luning of the background clutter.

Although not all the differences were significant, overall performance as measured by RT and accuracy tended to be best in the full overlap FOVs and worst in the partial overlap FOVs. There was no effect of target type. We had expected that since sharp targets are better dichoptic competitors, they would have shown superior performance. However, it may be that the clutter in our displays outweighed this factor. That is, FOV articulation caused by the contours from the

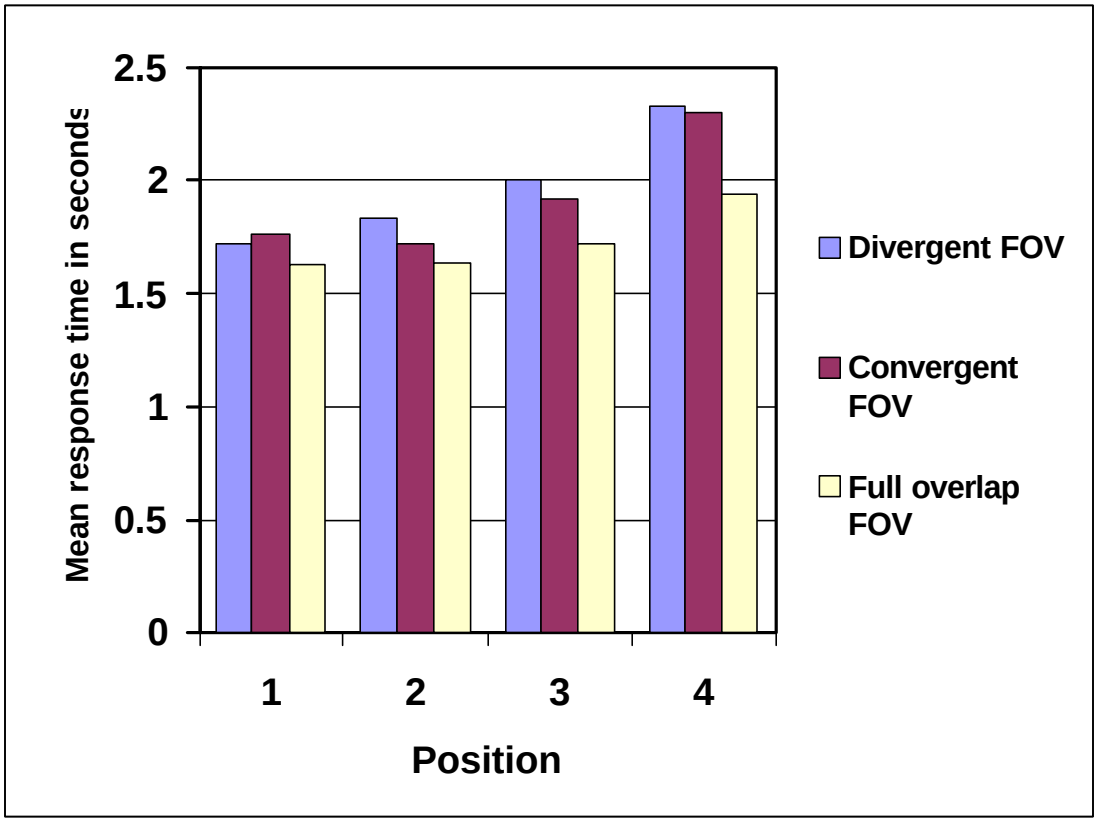

Figure 9. Mean RT to acquire target (FOV x Position).

clutter serves to lock in the correct competing image, and lock out the dark competing image from the incorrect eye, so that it does not come through in the binocular percept of the total FOV. Moffitt (1989) suggested that contours that occur in an FOV displaying a natural scene might eliminate luning and, presumably, the other detrimental effects such as the reduced visibility of targets that occur in partial binocular overlap displays. This occurs because the added contours bias the binocular rivalry in favor of the monocular image that contains the contours as opposed to the incorrect image which only contains a black featureless background and one contour, the binocular border (e.g., see Arditi, 1986; Anderson and Nakayama, 1994; Fox and Check, 1968, 1972; Fox, 1991; and Norman, Norman and Biotta, 2000). One would need to test visual search of targets in a clear uncluttered FOV to determine this. Performance, as expected, tends to get better over time as indicated by the block main effect and be better for positions closer to the center of the FOV as indicated by the position main effect. How much of an effect is due to the binocular border per se remains to be seen. Further research is needed to clarify these issues. In summary, on average, performance tended to be best in the full overlap FOV and poorest in the partial overlap FOVs, and the RT performance data were not disconfirmed by the two accuracy measures (number of errors and percent errorless target acquisition).

Table 2.
Number of errors ANOVAs.

Effect	Test	F	p-level
1. Block	F (5,100)	0.18	.97
2. FOV	F (2,40)	0.15	.86
3. Target	F (1,20)	3.49	.08
4. Position	F (3,60)	1.25	.30
5. Block x FOV	F (10,200)	0.73.	.69
6. Block x Target	F (5,100)	0.73	.60
7. FOV x Target	F (2,40)	0.03	.97
8. Block x Position	F (15,300)	1.03	.42
9. FOV x Position	F (6,120)	0.74	.62
10. Target x Position	F (3,60)	0.85	.47
11. Block x FOV x Target	F (10,200)	0.49	.90
12. Block x FOV x Position	F (30,600)	1.34	.11
13. Block x Target x Position	F (15,300)	0.98	.48
14. FOV x Target x Position	F (6,120)	0.60	.73
15. Block x FOV x Target x Position	F (30,600)	0.92	.60

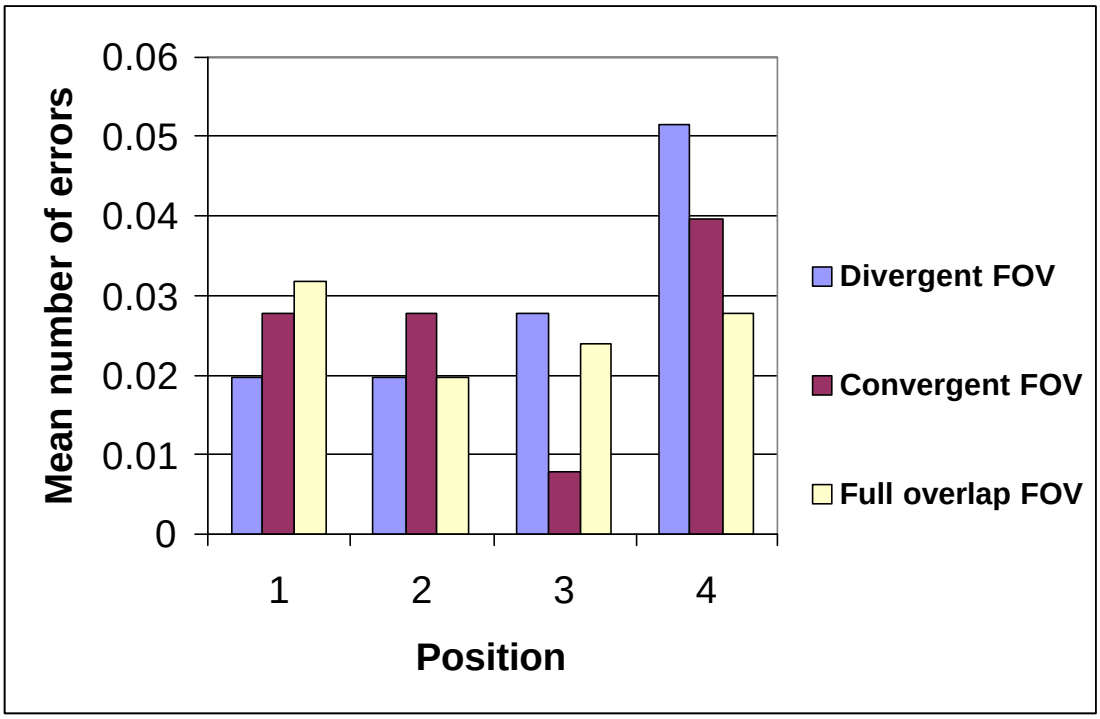

Figure 10. Mean number of errors per target acquired (FOV x Position).

Table 3.
Percent errorless target acquisition ANOVAs.

Effect	Test	F	p-level
1. Block	F (5,100)	0.17	.97
2. FOV	F (2,40)	0.65	.53
3. Target	F (1,20)	1.61	.22
4. Position	F (3,60)	1.39	.25
5. Block x FOV	F (10,200)	0.70	.72
6. Block x Target	F (5,100)	1.11	.36
7. FOV x Target	F (2,40)	0.39	.68
8. Block x Position	F (15,300)	0.80	.67
9. FOV x Position	F (6,120)	0.61	.72
10. Target x Position	F (3,60)	0.81	.50
11. Block x FOV x Target	F (10,200)	0.67	.75
12. Block x FOV x Position	F (30,600)	1.19	.23
13. Block x Target x Position	F (15,300)	1.42	.14
14. FOV x Target x Position	F (6,120)	0.86	.53
15. Block x FOV x Target x Position	F (30,600)	0.88	.65

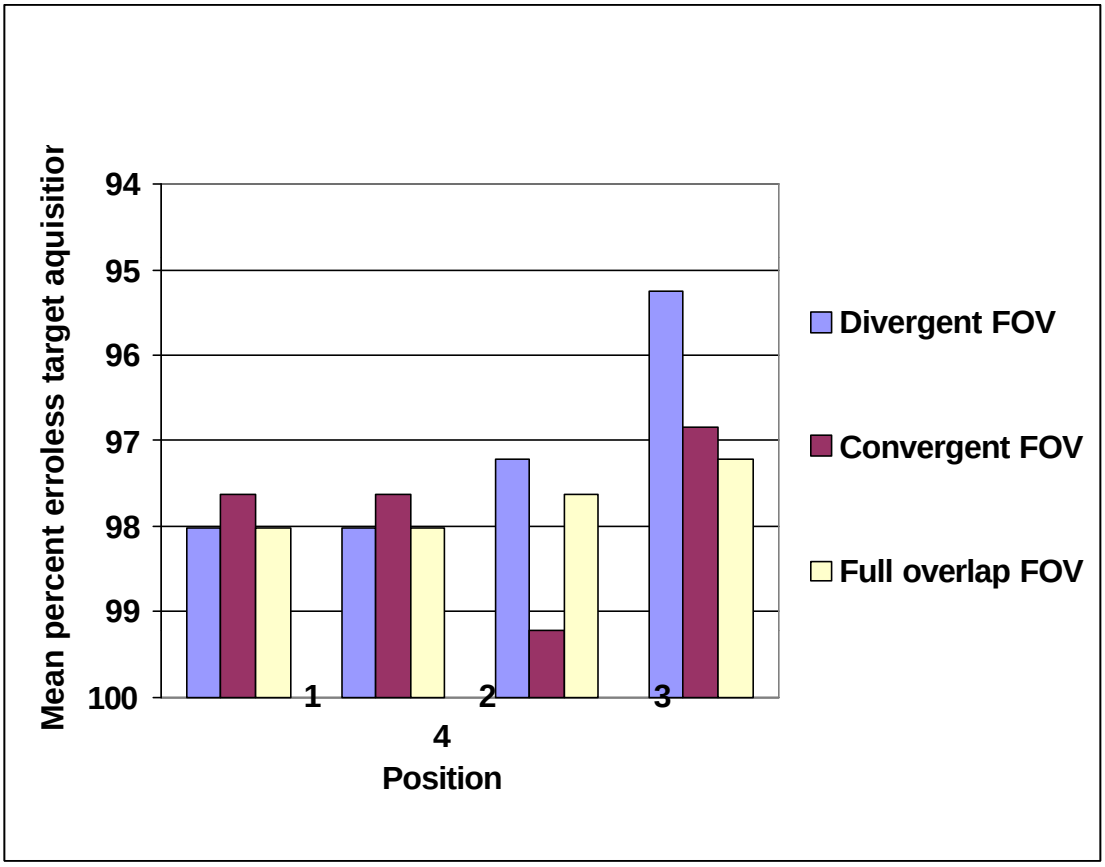

Figure 11. Mean percent errorless target acquisition (FOV x Position).

References

Alam, M. S., Zheng, S. H., Iftekharuddin, K. M., and Karim, M. A. 1992. Study of field-of-view overlap for night vision applications. Proceeding of the 1992 IEEE National Aerospace and Electronics Conference, NEACON Vol 3, 1249-1255. Dayton, OH.

Anderson, B. L., and Nakayama, K. 1994. Toward a general theory of stereopsis: Binocular matching, occluding contours, and fusion. Psychological Review, 101, No. 3, 414-445.

Arditi, A. 1986. Binocular vision. In (K. R. Boff, L. Kaufman, and J. P. Thomas) Handbook of perception and human performance, Vol. 1. New York: John Wiley & Sons.

Edgar, G. K., Carr, K. T., Williams, M., and Clark, A. L. 1991. The effect upon visual performance of varying binocular overlap. AGARD symposium on helmet-mounted displays and night vision goggles, Neuilly-sur-Seine, France. (AGARD Conference Proceedings 517), 8-1 to 8-15.

Fox, R. 1991. Binocular Rivalry. In (D. Regan) Vision and visual dysfunction, Vol. 9., 93-110.

Fox, R., and Check, R. 1968. Detection of motion during binocular rivalry suppression. Journal of experimental psychology, 78(3), 388-395.

Fox, R., and Check, R. 1972. Independence between binocular rivalry suppression duration and magnitude of suppression. Journal of experimental psychology, 93(2), 283-289.

Jennings, S., and Dion, M. 1997. An investigation of helmet-mounted display field-of-view and overlap tradeoffs. Proceedings of the Human Factors and Ergonomics, 41st Annual Meeting, 32-36.

Jennings, S., Dion, M., Srinivasan, R. and Baille S. 1997. An investigation of helmet-mounted display field-of-view and overlap tradeoff in rotorcraft handling qualities. 23rd European Rotorcraft Forum, 43.1-43.14.

Kaufman, L. 1963. On the spread of suppression and binocular rivalry. Vision research, 3, 401 - 415.

Kaufman, L. 1964. Suppression and fusion in viewing complex stereograms. American journal of psychology, 77, 193-205.

Kenyon, R. V., and Kneller, E. W. 1993. The effects of field of view size on the control of roll motion. IEEE transactions on systems, man, and cybernetics, 23(1), 183-193.

Klymenko, V., Harding, T. H., Beasley, H. H., Martin, J. S. and Rash, C. E. 1999. The effect of helmet mounted display field-of-view configurations on target acquisition. Fort Rucker, AL: U.S. Army Aeromedical Research Laboratory. USAARL Report 99-19.

Klymenko, V., Verona, R. W., Beasley, H. H., Martin, J. S., and McLean W. E. 1994a. Factors affecting fragmentation of partial binocular overlap displays. Fort Rucker, AL: U.S. Army Aeromedical Research Laboratory. USAARL Report 94-29.

Klymenko, V., Verona, R. W., Martin, J. S., Beasley, H. H., and McLean W. E. 1994b. Factors affecting the perception of luning in monocular regions of partial binocular overlap displays. Fort Rucker, AL: U.S. Army Aeromedical Research Laboratory. USAARL Report 94-47.

Klymenko, V., Verona, R. W., Martin, J. S., Beasley, H. H., and McLean W. E. 1994c. The effect of binocular overlap mode on contrast thresholds across the field-of-view as a function of spatial and temporal frequency. Fort Rucker, AL: U.S. Army Aeromedical Research Laboratory. USAARL Report 94-49.

Kruk, R., and Longridge, T. M. 1984. Binocular overlap in a fiber optic helmet mounted display. The image 3 conference proceedings, 363, 363-377. Brooks Air Force Base, TX: Air Force Human Resources Laboratory, Air Force Systems Command. AFHRL-TR-84-36.

Landau, F. 1990. The effect on visual recognition performance of misregistration and overlap for a biocular helmet mounted display. SPIE proceedings, Vol. 1290, helmet-mounted displays II, 173-184. San Jose, CA: SPIE-The International Society for Optical Engineering.

Melzer, J. E., and Moffitt, K. 1989. Partial binocular overlap in helmet-mounted displays. SPIE Proceedings, Vol. 1117, display system optics II, 56-62. San Jose, CA: SPIE-The International Society for Optical Engineering.

Melzer, J. E., and Moffitt, K. 1991. An ecological approach to partial binocular-overlap. SPIE proceedings, Vol. 1456, large screen projection, ionic, and helmet-mounted displays, 175-191. San Jose, CA: SPIE-The International Society for Optical Engineering.

Moffitt, K. 1989. Luning and target detection. San Jose, CA: Kaiser Electronics.

Moffitt, K. 1991. Partial binocular overlap: concepts, research, & systems. San Jose, CA: Kaiser Electronics.

Moffitt, K., and Melzer, J. 1991. Partial binocular overlap. San Jose, CA: Kaiser Electronics.

Norman, H. F., Norman, J. F., and Bilotta, J. 2000. The temporal course of suppression during binocular rivalry. Perception, 29(7), 831-841.

Osgood, R. K., and Wells, M. J. 1991. The effect of field-of-view size on performance of a simulated air-to-ground night attack. AGARD symposium on helmet-mounted displays and night vision goggles (AGARD Conference Proceedings 517), 10-1 to 10-7., Aerospace medical panel symposium, Pensacola, FL.

Wells, M. J., Venturino, M., and Osgood, R. K. 1989. The effect of field-of-view on performance at a simple simulated air-to-air mission. SPIE proceedings, Vol. 1116, helmet-mounted displays, 126-137. San Jose, CA: SPIE-The International Society for Optical Engineering.

Wolpert, L. 1990. Field-of-view information for self-motion perception. In (R. Warren and A. H. Wertheim) Perception and control of self-motion. Hillsdale, NJ: Lawrence Earlbaum Associates.